Available online at www.sciencedirect.com

ScienceDirect

journal homepage: www.elsevier.com/locate/bbe

Original Research Article

FPGA based real-time epileptic seizure prediction system

Ercan Cosgun [a], Anil Çelebi [b,*]

[a] University of Kirklareli, Vocational School of Technical Sciences, Electronics & Automation Department, Kirklareli, Turkey

[b] University of Kocaeli, Electronics and Telecommunications Engineering Department, Kocaeli, Turkey

ARTICLE INFO

Article history:
Received 16 October 2020
Received in revised form
21 January 2021
Accepted 22 January 2021
Available online 01 February 2021

Keywords:
Epileptic seizure prediction
Field programmable gate arrays (FPGA)
System-on-chip (SOC)
Electroencephalogram (EEG)
Hardware architecture
HW/SW co-design

ABSTRACT

The development of systems that can predict epileptic seizures in real-time offers great hope for epilepsy patients. These systems aim to prevent accidents that patients may experience caused by the loss of consciousness during seizures. Therefore, patients must use real-time epileptic seizure prediction systems that do not interfere with their daily activities. In this study, using the unipolar EEG data from a surface electrode, a patient-specific estimation system is implemented in real-time on a system on chip (SoC) that contains an embedded processor and programmable logic blocks. The European epilepsy database EPILEPSIAE is used in the scope of this work. In the proposed system, pre-processing is applied to the EEG data. Then, the features of the data in the frequency domain are extracted. The classifier model is trained with the RusBoosted Tree cluster classifier, which is a machine learning algorithm. Testing is carried out using the proposed classification model. Threshold values are determined, and then false alarms and erroneous classifications are prevented by post-processing. At the end of the tests, prediction success, sensitivity (SEN), Specificity (SPE), False Prediction Rate (FPR), and prediction times are obtained as 77.30%, 95.94%, 0.041 h^{-1}, and 33.23 min, respectively. The proposed system outperforms other studies in the literature in the number of electrodes, real-time operation, hardware/software architecture, and FPR performance. A wearable seizure prediction system seems to be commercialized according to the results achieved in this study.

1. Introduction

The World Health Organization(WHO) reports thtat there are over 50 million epilepsy patients worldwide [1,2]. Epilepsy is a nervous system disease characterized by the abnormal, sudden disruption of the electrical activity of brain cells, resulting in bizarre movements, sensory disturbances, and loss of consciousness [3]. The phase in which these disorders are seen is called a seizure. When this phase is over, the patient can continue his/her normal daily life. Common problems experienced by patients are loss of consciousness

* *Corresponding author at*: University of Kocaeli, Electronics and Telecommunications Engineering Department, Kocaeli, Turkey.
E-mail address: anilcelebi@kocaeli.edu.tr (A. Çelebi).

https://doi.org/10.1016/j.bbe.2021.01.006

during seizures and accidents caused by falls. Besides, the cause of stress to the patients comes from people's reactions and incorrect intervertion [4]. If patients knew they would have a seizure, they could have avoided activities that could cause them to have life-threatening accidents. Studies show that many seizures occur suddenly, but the initial phase (pre-ictal) can range from a few minutes to an hour [5,6]. In the literature, it has been suggested that the pre-ictal period of the patients should be determined as 50 min [7–9]. However, the findings we obtained in this study revealed that this period varies for each patient. Therefore, the preictal period for each patient has been selected specifically. The preictal period has been selected as 50 min for 5 patients, 60 min for another 4 patients and, 75 min for the remaining 1 patients.

EEG (Electroencephalogram) is the measurement of brain electrical activity with electrodes placed on the head surface or scalp. This measurement can also be performed invasively with electrodes placed in the brain tissue. EEG signal analysis is used as a diagnostic tool to detect pathologies associated with abnormal electrical behavior. Epilepsy disease is also detected by the interpretation of EEG spectra by experts in the relevant field [10]. The EEG signal of an epilepsy patient is divided into four sections: pre-ictal (before seizure), ictal (moment of seizure), post-ictal (after seizure), and interictal (inter-seizure). Preictal and interictal stages are the sections that are generally tried to be predicted in the scope of seizure prediction studies. According to researches, the preictal region contains sufficient information for seizure prediction [11,12]. In this study, the prediction process is carried out by classifying the pre-ictal and inter-ictal stages.

The general approach for epileptic seizure prediction and detection is as follows: Recording the EEG signal, pre-processing, extraction of features, and classification [13]. In some studies, it has been proposed to perform a post-processing phase to reduce classification errors [14]. All of the mentioned stages have been utilized in the scope of the proposed work.

The pre-processing phase consists of the segmentation of the EEG signal and the removal of network-borne noise. When the studies are examined, it has been observed that the segments which are going to be used in this process selected at different lengths of time slots. Segment lengths vary according to the methods and database used. While the segment length of 20 s was selected using the EPILEPSIAE database in Ref. [15], the segment length of 5 s was selected in Ref. [16], which uses the CHB-MIT database. In Ref. [17], the EPILEPSIAE database was used and a segment length of 5 s was chosen. To eliminate network-borne noise, a 50 Hz or 60 Hz notch filter was applied in some studies, depending on the database used [18]. Noise in EEG data is mostly caused by motor activities. To eliminate this noise, bandpass filters are generally used. In Ref. [19] a band-pass filter of 0.5−130 Hz was used. In Ref. [20] 0.1−100 Hz bandpass filter has been preferred. In [21] 50 Hz notch filter and 0.1−70 Hz bandpass filter have been used. In Ref. [22] instead of using a band-pass filter, the sliding average window method was used after feature extraction to eliminate this noise. In this study, the EEG signals are divided into 5 s segments, then a 50 Hz notch filter is used to eliminate the noise originating from the network.

EEG signals are mainly examined in five sub-bands. These are referred as delta (1–4 Hz), theta (4–7 Hz), alpha (7−12 Hz), beta (12−30 Hz), and gamma (30 Hz-) [23–25]. In Ref. [7], the gamma band is divided into five different sub-bands. These bands are defined as following: gamma1 (30−50 Hz), gamma2 (50−70 Hz), gamma3 (70−90 Hz), gamma4 (90−110 Hz) and gamma5 (110−128 Hz). In Ref. [26], except for the 5 sub-bands mentioned above, the raw data, 63 Hz, 100 Hz, and 200 Hz high-pass filter applied forms of the raw data are also considered as sub-bands. Thus, feature extraction was performed by using 10 subbands instead of 5. Derivatives of wavelet transform were used in some studies for subband separation [27]. Apart from these, studies in which the EEG signal is divided into sub-bands by performing frequency-time analysis with short-time Fourier transform and rational discrete short-time Fourier transform methods have also been proposed [28,29]. In Ref. [30], the EEG classification problem has been tried to be solved by transforming it into an image segmentation problem by using energy distribution in the time-frequency plane. Discrete wavelet transform without sub-sampling is used in Ref. [31] and wavelet coefficients are used as features. Thus, while obtaining wavelet coefficients, the signal length is kept constant at all levels. In some of the studies, the EEG signals have been separated into sub-bands called intrinsic mode functions (IMF) by using the empirical mode decomposition (EMD) method [32,33]. In Ref. [9], a performance comparison has been made between EMD and wavelet transform methods. In this study, the EMD method has been preferred for subband decomposition. In this work, EMD algorithm is provided to work in real time by using embedded processor and logic blocks. The details of hardware and software implementation of this method are discussed in detail in the following sections.

In machine learning, a measurable attribute is called a feature [34]. In the literature, many different algorithms have been proposed for extracting the features. In time domain, usually the skewness [6], kurtosis [16], mobility [17], variance [23], complexity and decorrelation time [24], standard deviation [33], mean [35], median and energy [36], autoregressive model(AR) coefficient [37], Shannon entropy [38] features have been extracted. In the frequency domain, features such as the energy of each subband decomposed [14], AR model coefficient [17], spectral power [22], spectral edge [23], relative spectral power, and absolute spectral power [7], for each sub-bands absolute mean, average power, standard deviation, kurtosis, ratio of the absolute mean [9], wavelet coefficient [36] and phase synchronization coefficient [39] have been extracted.

Apart from these, there are also studies making use of rule-based features [19,40]. Support vector machines (SVM) have been preferred as a machine learning algorithm in most of the studies [6,7,17,19,22,24,33,37,41]. In Ref. [42], SVM optimized with a genetic algorithm was used as the classifier. In Ref. [43], the classifier's accuracy has been increased by determining the SVM parameters with the grid search algorithm. Some studies used more than one classifier [44,45]. Apart from these, there are studies in which the random forest classifier is preferred [46,47]. In Ref. [48], different from the others, the classification was made using Neural Network Ensemble. Another classifier commonly used in the literature is cellular neural networks (CNN), which does not require features [18,27,35]. Apart from

these, some studies use more than one classifier and calculate performance criteria [9,14,23]. In Ref. [40], threshold values have been defined for the classification process. In Ref. [49], the classification process has been performed with the RusBoost classifier, which is mostly used on unbalanced data sets. In this study, the Rusboost Tree classifier algorithm was chosen as the classifier since the model was trained without equalizing the number of observations of the classes.

Postprocessing is a frequently used method to avoid false alarms caused by classification errors. Researchers have proposed different methods as post-processing. False alarms have been prevented by using Firing power (*fp*) in Refs. [14,23]. In Ref. [50], final processing has been done by looking at power and energy attributes. In Ref. [51], by looking at the last 10 samples of the classification output with 0.5-sec intervals, a warning rises according to the threshold value determined for each patient. In this study, FP was preferred and the final procedure was performed using the threshold values determined for each patient. Thus, false alarms are prevented.

Field Programmable Gate Arrays (FPGA) are integrated circuit chips that the designer can reprogram on the field. With the addition of hardcore embedded processors to these chips, hybrid structures, also called System-on-Chipemerged. In recent studies, it has been shown that real-time embedded systems can be implemented [36,40,52]. The hardcore processors are usually utilized to perform control-based functions. On the other hand, the programmable logic part of the SoC is utilized to implement time-sensitive complex data path operations of the method that is being implemented [53]. Evaluation boards using such chips are usually preferred for the development phase of any method. A custom processing board is developed after promising results are achieved. Such an evaluation board that contains an SoC with integrated processor cores (PS) and programmable logic (PL) has been used to implement the hybrid hardware-software (HW/SW) architecture proposed in this work.

In this study, a real-time epileptic seizure prediction system with a hybrid HW/SW architecture is proposed. The European Epilepsy Database - EPILEPSIAE has been used in the scope of the work. Unlike previous studies, a machine learning algorithm and hardware architecture is proposed to perform seizure prediction on the signal received from a single EEG electrode as unipolar. Thanks to this study, for the first time in the literature, classification has been made on the hardware by using the RusBoosted Tree classifier with the unbalanced data set. In the study, patient-based threshold values were determined and classification errors were reduced. The results of the study show that an epileptic seizure can be successfully predicted in realtime by using a single EEG electrode.

Various studies have been carried out on wearable systems in the healthcare field [54–56]. Likewise, there are also wearable system studies on epilepsy disease in the literature [57–61]. A wearable system should be designed in such a way that it does not affect the living standard of the patient during use. In this case, one of the most important features of a wearable system to be designed for epilepsy disease should be as few electrodes as possible on the system because the patient will carry such a system around the skull throughout the day. One of the critical problems faced by epilepsy patients is the uneasiness they experience due to the risk of seizures in daily life. This situation is one of the most important problems in the social life of epilepsy patients. In this direction, within the scope of the proposed study, considering the developments in the field of EEG sensors, it is aimed to use a single electrode. Thus, it is aimed to develop a system that will cause the least visual difference in the body of a patient and which is low in attention.

The rest of the paper is organized as follows. In Section 2, the EPILEPSIAE database is being introduced; information about the pre-processing stage, EMD, feature extraction, classification, post-processing, hardware architecture, and performance parameters are given. Experimental results, comparison with other studies, the selection process of the right channel, and the determination of the threshold values are mentioned in Section 3. The conclusions are discussed in Section 4.

2. Materials and methods

The training of the designed classifier has been carried out on a personal computer (PC). Tests have been performed using both the development board which contains the SoC and the PC. The reason for using both platforms for the test is to understand that the HW/SW architecture proposed for seizure prediction matches the PC implementations as illustrated in the block diagram in Fig. 1.

2.1. *The EEG dataset*

The EPILEPSIAE database has been defined as the most comprehensive dataset containing the EEG data of 275 patients in the literature [62–64]. Only 30 patients' EEG data of this data

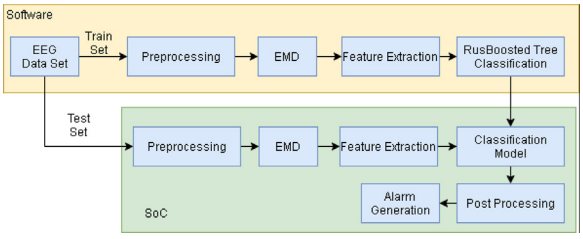

Fig. 1 – Block Diagram of the proposed epileptic seizure prediction system.

Table 1 – Summary of the dataset used in this paper.

Patient Code	Patient ID	Focus	Seizure Type	Number of Seizure	Recording Length (Hour)
FR_110	PAT1	T, Right	UC, CP, SP	8	143
FR_89	PAT2	T, Left	UC, CP	5	167
FR_239	PAT3	T, Left	SP	5	118
FR_308	PAT4	T, Right - T, Left	SP	9	159
FR_327	PAT5	T, Right - T, Left	CP	6	166
FR_454	PAT6	T, Right - T, Left	CP,SP	5	118
FR_467	PAT7	T, Right	SP,CP,SG	6	92
FR_591	PAT8	T, Right	SP,CP	7	164
FR_852	PAT9	54	CP,UC	10	94
FR_1119	PAT10	42	SG,UC,SP	8	159
Total					1380

T: Temporal, C: Central, UC: Unclassified, CP: Complex Partial, SP: Simple partial, SG: Secondarily Generalized.

set are available to the users [64]. 10 patients' EEG data among 30 are utilized in the scope of this work. One of the criteria used for selecting a patient is the availability of long records taken at once. Thus, it was aimed to minimize the problems that may arise from measurement differences by using a long recording taken from the same electrode at one time instead of short recordings taken from the same electrode at different times. The use of non-invasive measurement results is another criterion adopted in patient selection. The reason for this is that it is aimed to develop a system that can be easily used within the scope of the proposed study. The electrode that gives the most successful prediction result varies from patient to patient. EPILEPSIAE dataset contains EEG data of 19 channels captured via 10–20 electrode placement system with 256 Hz sampling rate. The epileptic region, seizure onset, and seizure end times are marked by experts, provided within the database. The information of the patients whose EEG data are used is shown in Table 1. In Fig. 2, 2 h of EEG data of PAT2's F7 channel is presented.

2.2. *Pre-processing*

This process consists of data segmentation and 50 Hz notch filtering. The data is divided into chunks of 5 s each to calculate the features used for seizure prediction. The reason for choosing the length of 5 s is the effective use of FPGA memory limited to several Megabits within the chip. The purpose of using the 50 Hz notch filter is to eliminate the noise originating from the electrical network.

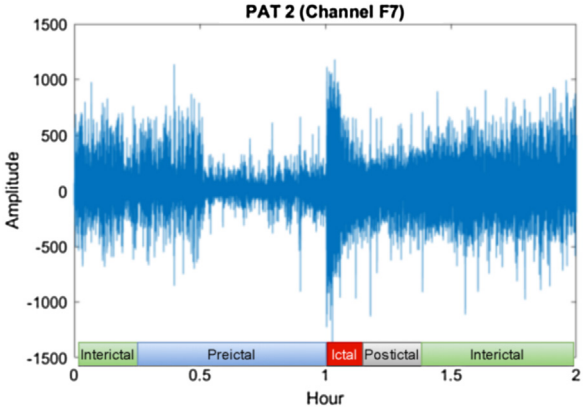

Fig. 2 – Two hours long EEG data of PAT2.

2.3. *EMD*

EMD is the signal separation method used for linear and non-stationary signals such as EEG signals [65]. In this method, signals are decomposed into subcomponents called IMF. Each IMF represents oscillations in specific frequency ranges. The flow diagram of the EMD method is illustrated in Fig. 3. To implement such computationally demanding and iterative algorithms on mobile platforms, high memory bandwidth and processing power are required [66]. Thus, the EMD method is divided into control and data path operations. In the scope of the proposed work, the HW/SW architecture is implemented in the PS and PL portions of the SoC device respectively.

EMD function is performed in 3 stages. Local maximum and local minimum values are determined first. The lower and upper envelopes of the signal are calculated using the cubic spline interpolation process. The difference between the original signal ($x(t)$) and the average envelope ($m(t)$) is determined as the candidate IMF ($h^k(t)$) by taking the average of the lower and upper envelopes obtained in the interpolation process as illustrated in Eq. (1).

$$h^k(t) = x(t) - m(t) \tag{1}$$

To decide whether the obtained candidate IMF is the real IMF or not; the *Cauchy* type convergence criterion, one of the sifting termination criteria, is examined [67]. This stopping decision value SD is set at 0.2 at [68]. The sieving process continues until the SD is less than 0.2 or until it reaches the number of specified cycles(In the study, 100 was determined as the number of cycles). When the error termination criteria are met, the candidate IMF is determined as the real IMF and removed from the original signal. SD is calculated as in Eq. (2).

$$SD = \frac{\sum_{t=0}^{T} (h_{k-1}(t) - h_k(t))^2}{\sum_{t=0}^{T} (h_{k-1}(t))^2} \tag{2}$$

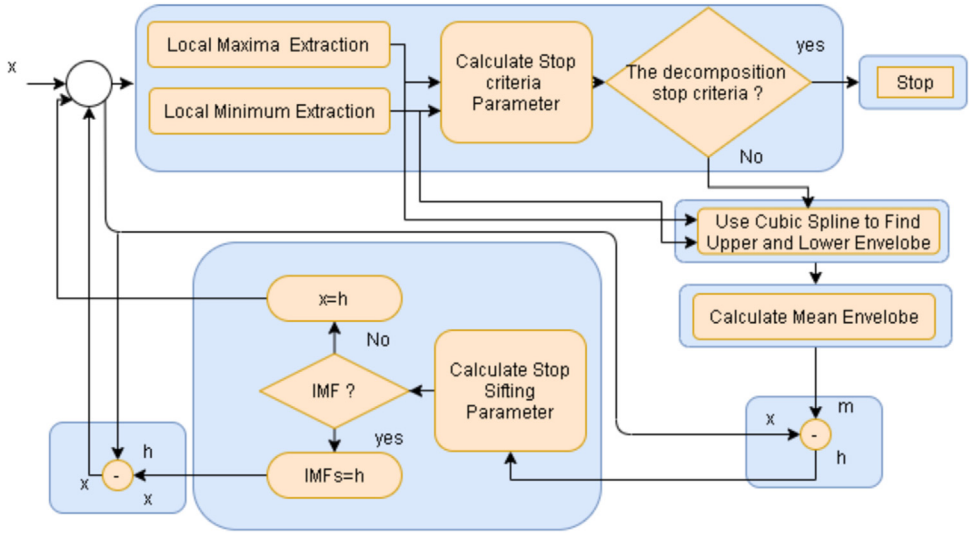

Fig. 3 – EMD flow diagram.

The following two conditions determine whether there is a new IMF in the remaining signal;

- First condition; If *EnergyRatio* (the ratio of the original signal x (t) to R_Sig (t), which is the remaining signal from the k. IMF) is greater than 20, it is decided that there is no new IMF [69]. This ratio is calculated in dB as in Eq. (3).

$$\text{EnergyRatio} = 10log_{10}\frac{x(t)^2}{R\_Sig(t)^2} \quad (3)$$

- The second condition is that if the sum of the local largest and local smallest numbers of the signal is less than 1, it is decided that there is no new IMF.

In the last case, if there is no new IMF to be calculated, the original signal is determined as the sum of the IMFs and the remaining signal (h). Eq. (4) gives the expression of the original signal in terms of IMFs and the remainder signal.

$$x(t) = \sum_{i=1}^{n} imf(t) + h(t) \quad (4)$$

By examining previous studies, it was determined which IMFs the frequency bands of the EEG signals correspond to and are given in Table 2 [6,70]. When Table 2 is examined, it is seen that the first 5 IMFs represent all sub-bands of the EEG signal used. For this reason, only the first 5 IMFs of the signal are calculated in the scope of the proposed work.

The first 5 IMFs of the 5-second EEG signal chunk are shown in Fig. 4a and the frequency spectra of these IMFs are shown in Fig. 4b. In Fig. 4a, the x-axis shows the time and the y axis shows the amplitude of each IMF. In Fig. 4b, the x-axis represents the frequency and the y axis represents the power respectively.

2.4. *Feature extraction*

It has been observed in the literature that, many linear and non-linear features are used by researchers. In this study, the following features, which are frequently preferred in the literature, are used and calculated for each IMF. So, 85 features are calculated in total for 5 IMFs where 17 features are used for each IMF as illustrated in Table 3. In Table 3, *F*, *IMF*, and *x* represent the features, intrinsic mode functions, and input signal respectively.

2.5. *Classification*

Most of the machine learning algorithms work with the assumption that there is an equal number of observations for each class within a data set. If the number of observations for each class within a data set is not equal, that kind of data set is considered to be an unbalanced data set. When a classification is performed with a classical machine learning algorithm on such a dataset, the class with less number of observations will

Table 2 – Equivalent of Subband in IMFs.

IMFs	Frequency Range (Hz)	EEG Rhythm	Defined Frequency Range (Hz)
IMF1	(40Hz-]	Gamma	(35Hz -]
IMF2	(15–40 Hz]	Beta	(18–35 Hz]
IMF3	(6–15 Hz]	Alfa	(7–18 Hz]
IMF4	(2–5 Hz]	Teta	(4–7 Hz]
IMF5	(- 2Hz]	Delta	(- 4 Hz]

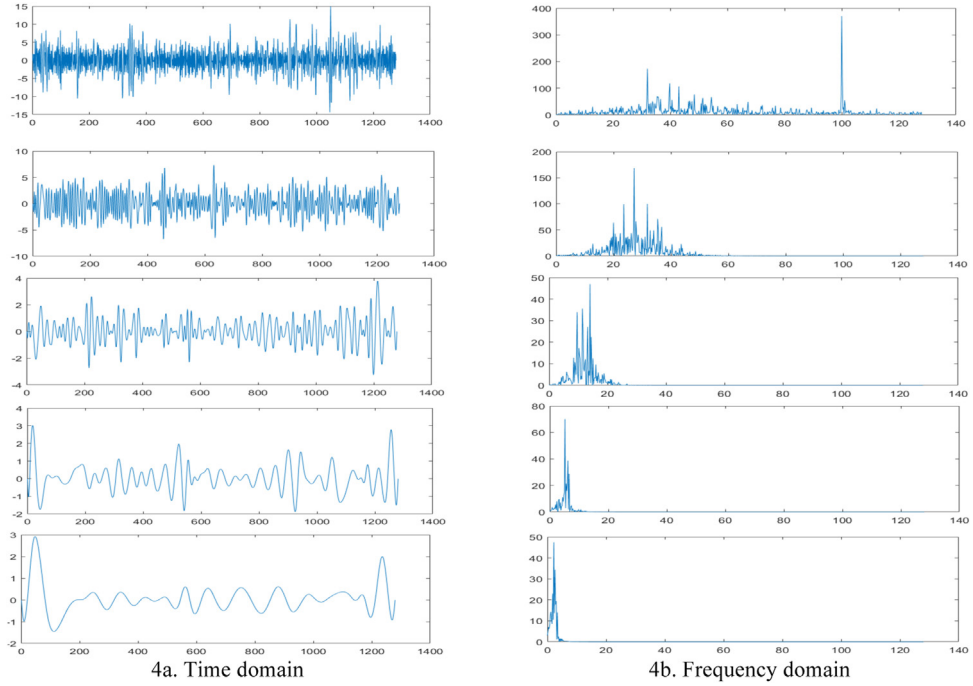

Fig. 4 – First 5 IMFs.

be overlearned. In this study, the RusBoosted Tree classifier, which provides promising classification performance on unbalanced data sets, is preferred [71]. The RusBoosted classifier is preferred when the imbalance rate between classes is very large. Furthermore, it also uses a subsampling strategy to shorten the training time. Thus, it performs the classification process without losing considerable information. The training of the proposed system has been carried out on the PC and tests have been carried out on the SoC. The 5 folds cross-validation approach is used in the training [72,73].

The RusBoosted classifier approach given in Fig. 5 is based on principle of randomly removing samples from the many classes until the desired balance is achieved by using subsampling. In the RusBoosted method, a new classifier is

Table 3 – List of Features.

Features	Equation	Features	Equation
Absolute Mean:	$F_{1-5} = \sum_{i=1}^{n} \frac{\lvert IMF_i \rvert}{n}$ (5)	Mobility	$Mean'_y = \sum_{i=1}^{n-1} IMF'_i$ (15)
Mean	$F_{6-10} = \sum_{i=1}^{n} \frac{IMF_i}{n}$ (6)		$F_{51-55} = \sqrt{\frac{\Sigma_{i=1}^{n-1} \frac{(IMF'_i - Mean'_y)^2}{n-1}}{F_{11-15}}}$ (16)
Variance	$F_{11-15} = \sum_{i=1}^{n} \frac{(IMF_i - F_{6-10})^2}{n-1}$ (7)	Complexity	$Mean''_y = \sum_{i=1}^{n-2} IMF''$ (17)
Standard Deviation	$F_{16-20} = \sqrt{\sum_{i=1}^{n} \frac{(IMF_i - F_{6-10})^2}{n-1}}$ (8)		$M'_y = \sqrt{\frac{\Sigma_{i=1}^{n-2} \frac{(IMF''_i - Mean''_y)^2}{n-2}}{\Sigma_{i=1}^{n-1} \frac{(IMF'_i - Mean'_y)^2}{n-1}}}$ (18)
Sum	$F_{21-25} = \sum_{i=1}^{n} IMF_i$ (9)		$F_{56-60} = \frac{M'_y}{F_{51-65}}$ (19)
Energy	$F_{26-30} = \sum_{i=1}^{n} IMF_i^2$ (10)	Shannon Entropy	$F_{61-65} = -1 \times \sum_{i=1}^{n} IMF_i \times \log_2(IMF_i)$ (20)
Band Power	$F_{31-35} = \frac{\Sigma_{i=1}^{n} IMF_i^2}{n}$ (11)	Shannon Energy	$F_{66-70} = \sum_{i=1}^{n} \log_2(IMF_i)$ (21)
Root mean square(RMS)	$F_{36-40} = \sqrt{\frac{\Sigma_{i=1}^{n} IMF_i^2}{n}}$ (12)	Normalized Spectral Power	$F_{71-75} = \frac{\Sigma_{i=1}^{n} (IMF_i)^2}{\Sigma_{i=1}^{n} x_i^2}$ (22)
Kurtosis	$F_{41-45} = \frac{\Sigma_{i=1}^{n} \left(\frac{IMF_i - F_{6-10}}{n}\right)^4}{(F_{16-20})^4}$ (13)	Max	F76–80 = (Maximum value of each IMF)
Skewness	$F_{46-50} = \frac{\Sigma_{i=1}^{n} \left(\frac{IMF_i - F_{6-10}}{n}\right)^3}{(F_{16-20})^3}$ (14)	Min	F81–85 = (Manimum value of each IMF)

′ : *First Order Deri*, ″ : *Second Order Deri.*

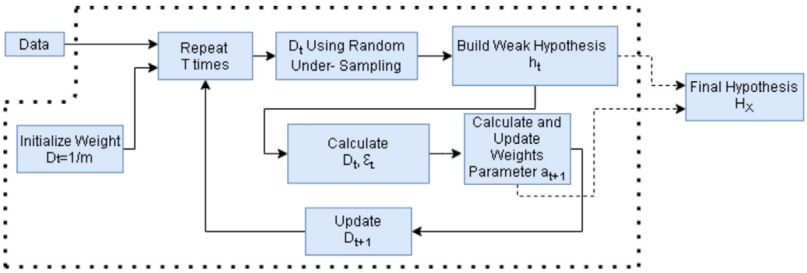

Fig. 5 – Rusboosted Classification Approach.

trained in each iteration to identify misleading observations. In the first step, equal weights are assigned to each sample. In Fig. 5, m represents the number of samples, t represents the number of iterations between 1 and T (the number of the ensemble classifiers), D_t represents the weight distribution of the sample. In this study, the decision trees method is used as a classifier model. The classifier model obtained is called h_t weak hypothesis. Then, the so-called error ε_t is calculated according to weight distribution, and a_{t+1} and D_{t+1} are updated depending on ε_t. This process is repeated T times so that the number of samples in the majority class approaches the number of samples in the minority class. At the end of the iterations, the final classifier model H_x is obtained according to the weighted voting result among the weak hypotheses (classifiers). The details of this algorithms is presented in Ref. [74].

2.6. *Post-processing*

High sensitivity is expected from epileptic seizure prediction systems. Classification errors mostly depend on the different characters of the attacks or the actual physiological condition of the patient. Classification error is a serious problem for seizure prediction. False alarms may occur due to classification errors. In this study, Firing Power (fp) method, which is a moving average technique, is used as a -post-processing step to reduce the number of false alarms [15].

$$fp[n] = \frac{\sum_{k=n-t}^{n} o[k]}{t} \tag{23}$$

Here *fp[n]* shows the firing power value at the *n*th discrete-time, *t* represents the number of samples at a preictal time and *o[k]* shows the classifier output. For example, for a 50-minute pre-ictal region, *o[k]* contains the classifier output for the last 600 segments and a new *fp* value is calculated every 5 s. Here, *o[k]* takes the value 0 (interictal) or 1 (preictal). *fp[n]* takes values ranging from 0 to 1. There are two conditions for the system to generate an alarm:

- Condition 1: 3 thresholds (TH1, TH2, and TH3) are determined iteratively for each patient. For an alarm to occur, the *fp[n]* value is expected to rise above TH1 and then TH2. For the system to generate a new alarm, again, *fp[n]* must go below TH1.
- Condition 2: It takes a certain amount of time for *fp[n]* to increase from TH1 to TH2. This threshold value is called TH3. Thus, the number of false alarms that occur in sudden changes of fp is reduced.

2.7. *Hardware-software architecture*

The test of the proposed system is carried out on a development board. The board has an SoC chip manufactured in 45 nm technology that contains both an embedded processor and programmable logic fabric. To achieve real-time operation, a digital circuit is designed so that the components with high processing load run in the programmable logic unit, and software is implemented to perform the control portion of the prediction system on the embedded processor core. The suggested hardware architecture for this study is shown in Fig. 6. PL refers to the programmable logic unit and PS refers to the embedded processor.

Communication with the development board is provided via the PC using UART (115,200 baud rate). *Buffer* block seen on PS is used to avoid data loss. Buffer has two arrays with 1280 elements named *Buff1* and *Buff2* and works in a ping-pong structure. When any buffer is full, Notch filter, *IP_Local_MAx_Min*, and *IP_Cubic_Spline* functions are executed respectively in PS. These functions prepare the necessary data and send it to PL, and the circuit on the PL calculates IMFs and sends it to PS back. Then, extracted features are applied to the classifier. The result generated by the classifier model is given as an input to the firing power function. If the necessary conditions are met, an alarm is generated. The calculated results are transferred to the PC back via UART.

The blocks named with IP prefix (IP_Cubic_spline, IP_Local_Max_Min) operate in PL. These cores are developed with a high-level synthesis (HLS) approach and implemented on FPGA. The bus interface to integrate the hardware cores with the embedded processor is also developed with the HLS approach. The software components of the prediction algorithm are coded in C / C ++ to be run on the embedded processor, including the communication functions to interact with intellectual property (IP) cores in PL.

IP_Local_Max_Min: This core calculates the indices of the local maximum and local minimum values of $x(t)$. The input and output of this core are connected to the processor within a streaming form. In the streaming data interface, there is a memory buffer to provide uninterrupted data flow between PL

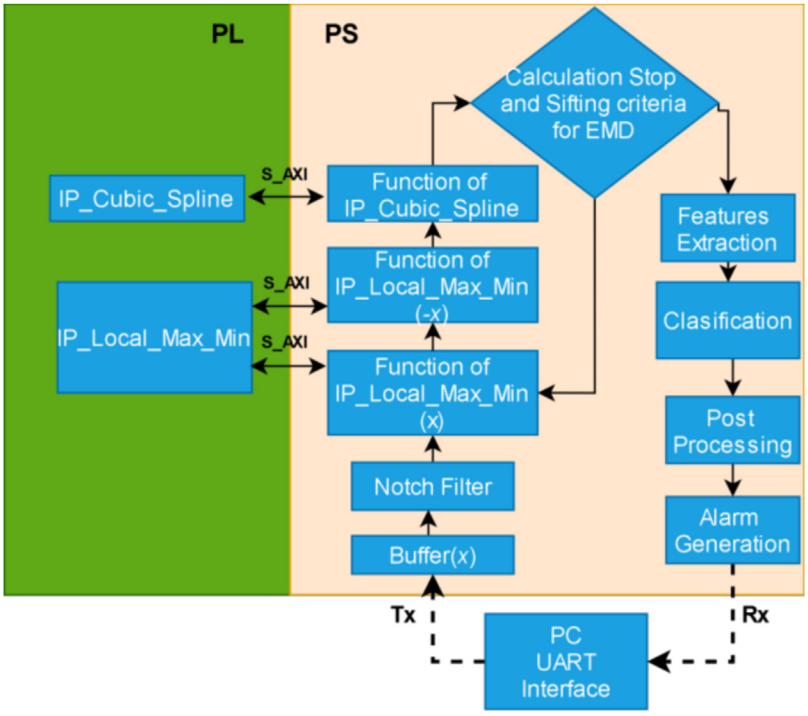

Fig. 6 – Hardware Architecture.

and PS sections. The architecture of this core is illustrated in Fig. 7.

The architecture illustrated in Fig. 7 consists of 4 blocks. These blocks determine the indices where the slope of the signal is zero, by calculating the second-order derivative of the input signal [75]. Step 4 block in the architecture is calculating the decision of whether the current index is a local maximum or not, by checking the second derivative value of the input signal. The input signal is negated before being driven into the kernel for calculation of local minimum indices.

IP_Cubic_Spline: This IP core performs the cubic spline interpolation process within the local minimum and local maximum values provided by the embedded processor core within a data stream form as explained before. The signal produced by this kernel is required for the calculation of upper and lower envelopes. Cubic spline interpolation is the name given to a flexible strip form made up of third-order polynomials that pass-through n control points. Details of this method are described in Ref. [65]. Normally, a straight line passes through two points. However, by fitting a 3rd order polynomial with cubic interpolation, it is aimed to provide a smoother curve combination. The general formulae of these polynomials are given in Eq. (24). The hardware architecture of this IP core is illustrated in Fig. 8.

$$S(x) = a_j + b_j \times (x - x_i) + c_j \times (x - x_j)^2 + d_j \times (x - x_j)^3 \quad (24)$$

Here, j represents indices continuing from 0 up to n-1, a_j, b_j, c_j and d_j represent the polynomial coefficients and, x_j represents control points. The purpose here is to find the coefficients of the 3rd order polynomial between two control points. In this case, the following conditions are met.

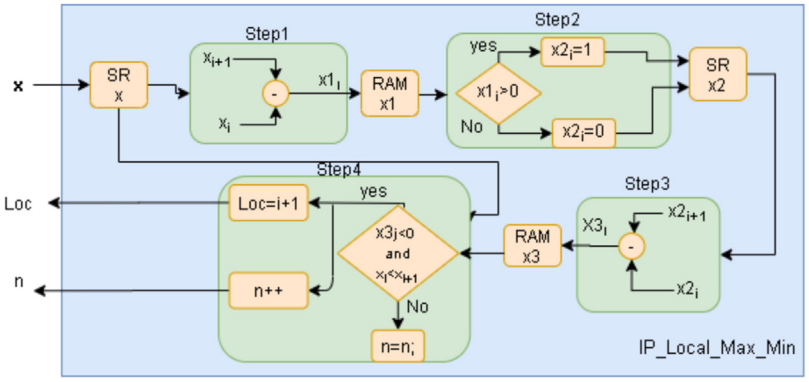

Fig. 7 – IP_Local_Max_Min architecture (SR: Shift Register).

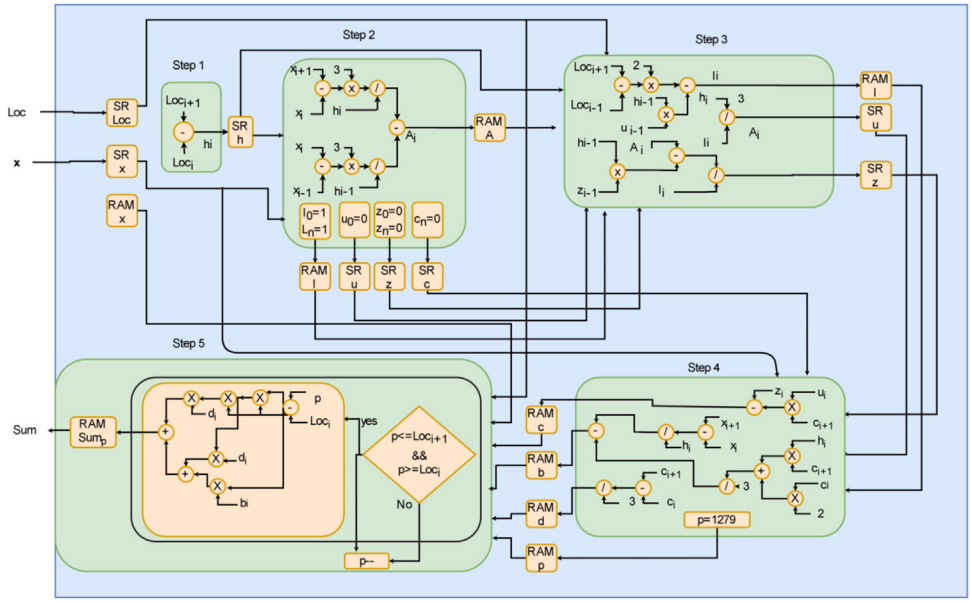

Fig. 8 – IP_Cubic_Spline architecture (SR: Shift Register).

In Fig. 8, the coefficients a, b, c, and d of step 2, step 3, and step 4 were found using the *Crout* decomposition method as in Ref. [76]. Thus, less resource utilization is achieved.

2.8. *Performance evaluation*

When the epileptic seizure prediction studies in the literature are examined, it has been seen that parameters such as Sensitivity (SEN), FPR, and average prediction time are used to measure the test performance. *SEN*, as shown in Eq. (25) is expressed as the number of alarms generated by the system divided by the total number of seizures. Additionally, the SEN of a test is also called the true positive rate (TPR).

$$SEN = \frac{Number\ of\ Generated\ Alarm\ (TP)}{Number\ of\ Total\ Seiures\ (TP + FN)} \times 100 \tag{25}$$

FPR is the number of false alarms per hour (Eq. (26)).

$$FPR = \frac{Number\ of\ False\ Alarm\ (FP)}{Hours\ of\ Testing - (\ preictal\ time \times number\ of\ seziures)} \tag{26}$$

In some studies, specificity (SPE) has also been included in performance parameters (Eq. (27)).

$$SPE = \frac{TN}{TN + FP} \tag{27}$$

TP, FN, FP, and TN parameters in the equations Eq. 25, Eq. 26, and Eq. 27 show: the number of correct alarms that have occurred in the pre-ictal period, the number of false alarms that have not occurred in the pre-ictal period, the number of false alarms that have occurred outside the pre-ictal period, and the number of correct alarms that have not occurred at the beginning of the pre-ictal period. Fig. 9 shows how TP, FN, FP, and TN expressions are defined according to firing power output. The dashed green lines shown in Fig. 9 represent the pre-ictal onset time and the red dashed lines represent the ictal onset.

In addition to these, Seizure Occurrence Period (SOP) and Seizure Prediction Horizon (SPH) parameters were also used as success criteria in some studies. SOP is defined as the time interval in which a seizure is expected to occur. SPH is the time between an alarm generated and the start of the SOP. For an alarm to be considered correct, the attack must occur after SPH and within the SOP. It is also defined as SPH intervention time. In short, if an alarm has risen in the system, it means that the seizure will occur after the SPH time at the earliest and after the SOP + SPH time at the latest. SOP and SPH periods are shown in Fig. 10.

In this study, to test the performance of the system, SEN, SPE, FPR, and the average parameters have been used as success criteria, taking into account the SOP and SPH periods.

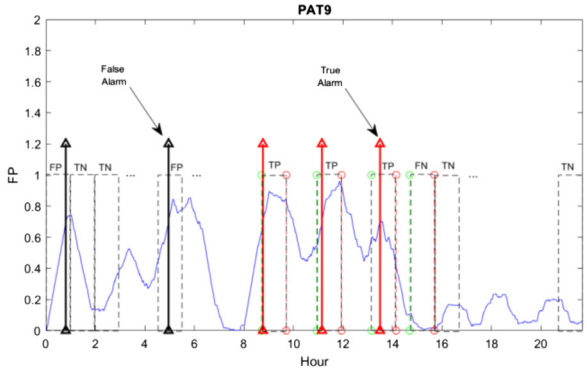

Fig. 9 – Test results for PAT9.

Fig. 10 – Demonstration of SOP and SPH periods.

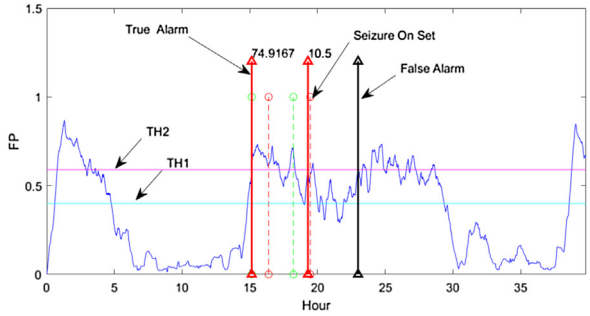

Fig. 11 – PAT5 hardware test results.

3. Results

In this section, the results of the proposed seizure prediction system are explained. In this study, 10 patients were classified using single electrode EEG data of The European Epilepsy Database. Long recordings that were not used while creating the classification model were tested on the proposed hardware architecture for a total of 507.8 h.

Fig. 11 shows the FP output of the patient PAT5's test data. Here, the dashed red line indicates the beginning of the seizure. The dashed green line represents the beginning of the SPH + SOP (Pre-ictal Period). For an alarm to be considered correct, it must be generated within the time slot that starts by the green dashed line(SPH) and ends by the point that is 5 min before the dashed red line (SPH + SOP - 5). Apart from these, the generated alarms are considered false alarms, and the FPR equation is calculated as in Eq. (26). SEN, SPE, and FPR parameters of other patients were calculated according to these criteria (Table 4).

In Table 4, recording times, the number of seizures used for training and testing, preictal time, SPH, threshold values, sensitivity, specificity, average prediction times, FPR values are presented. According to the experimental results, the average sensitivity of 77.3%, the average specificity of 95.94%, the prediction success of 76.9% (20 seizures out of 26), the mean FPR of 0.041 $h^{-1,}$ and the average prediction time of 33.23 min have been achieved.

The proposed method has been successfully implemented on the SoC and FPGA development board. The resource utilization of the proposed hardware architecture is presented in Table 5. There are 4 fundamental building blocks in an FPGA: block random access memories (BRAM) to implement the memory, DSP48E blocks to implement high speed multiplication operations, flip-flops (FF) to synchronize the internal and external signals to the system clock signal, lookup tables (LUT) to implement logic or datapath functions.

4. Discussion

In this section, the results of the proposed epilepsy prediction system are examined and compared with the previously proposed studies. Performance parameters, FPR, and SEN are required to be 0 and 100 respectively. Unfortunately, achieving accurate precision is not possible. One's improvement leads to the deterioration of the other. For this reason, the threshold values were optimized by considering these two parameters. TH1 and TH2 values are determined for each patient by the iterative trial and error method. TH3 value is the segment value determined to prevent rising alarms during sudden transitions to TH1 and TH2 values. For example, the TH3 value of PAT5 is determined as 150 segments. Since each EEG data chunk is 5 s in length, the transition time from TH1 to TH2 must be at least 12.5 min to generate an alarm for the patient

Table 4 – Hardware test results of the proposed algorithm.

Patient ID	Test Recording Time (Hour)	Number of Seizures (Train)	Number of Seizures (Test)	Preictal Period (Min.)	SPH (Min.)	TH1	TH2	TH3	Number of true Alarm	SEN (TPR) %	SPE %	Mean Prediction Time Before Seizure (Minutes)	FPR h^{-1}
PAT1	40.53	5	3	50	5	0.08	0.1	60	2	66	97.80	**13.28**	0.025
PAT2	32.81	3	2	60	5	0.29	0.39	50	2	100	100	36.79	0
PAT3	46.35	3	2	50	5	0.59	0.73	200	1	50	98.13	38.25	0.021
PAT4	49.40	6	3	60	5	0.87	0.89	20	2	66	100	43.58	0
PAT5	39.83	4	2	75	5	0.4	0.59	150	2	100	96.65	42.70	0.02
PAT6	45.85	3	2	60	5	0.18	0.44	300	2	100	95.43	39.37	0.045
PAT7	35.71	4	2	50	5	0.24	0.3	150	1	50	95.10	20.08	0.058
PAT8	114.22	4	3	50	5	0.82	0.91	40	3	100	92.54	26.94	0.08
PAT9	21.68	6	4	60	5	0.46	0.7	30	3	75	94.34	**47.6**	0.048
PAT10	81.4	5	3	50	5	0.04	0.09	30	2	66	89.43	22.66	0.136
Total	**507.80**	**43**	**26**						**20**				
Mean										**77.30**	**95.94**	**33.23**	**0.041**

Bold values represents total and average values.

Table 5 – Hardware Performance Evaluation.

Hardware Block	BRAM_18K (%)	DSP48E (%)	FF (%)	LUT (%)
IP_Cubic_Spline	18	50	18	55
IP_Local_Max_Min	11	2	2	7
Total:	29	52	20	62

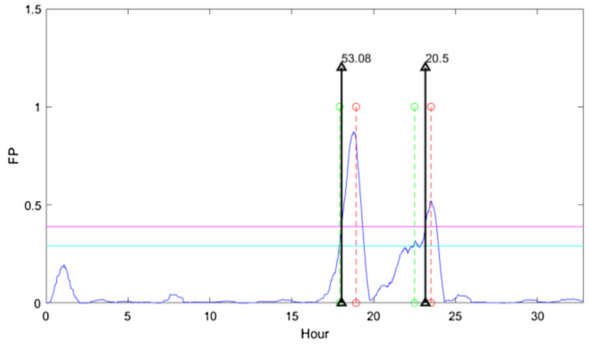

Fig. 12 – Result of Test (PAT2).

PAT5. When Fig. 11 is examined, an alarm is expected to be generated within 5 h according to the value of TH1 and TH2. However, if this transition time between two threshold values is below 12.5 min, the system does not generate an alarm. Thus, the number of false alarms has been reduced.

Correct alarms have been generated at least 5 min before the seizure for all patients. Therefore, the SPH value has been determined as 5 min. The preictal period (SOP + SPH) has been determined as 75 min in PAT5, 60 min in PAT2, PAT4, PAT6, and PAT9, and 50 min in other patients. It is concluded that these periods are affected by the character of the seizure or the quality of measurement. As an example, when looking at Fig. 12, it is seen that the FP value for PAT2 begins to meet the TH1 and TH2 conditions in less than 50 min. In this context, the preictal period value for PAT2 is determined as 60 min, which is the best value close to 50 min. At the beginning of the study, this period was predicted to be 50 min for all patients. However, experimental studies have revealed that this period varies for each patient.

Channel selection has been made by looking at the power values of the ictal times. The average seizure power is calculated for each EEG channel of a patient. The channel representing the pre-ictal and having the highest power value is selected. In Fig. 13, it is seen that the channel with the highest power belonging to PAT5 is channel 8 (P4). The selected EEG channel list for other patients is presented in Table 6.

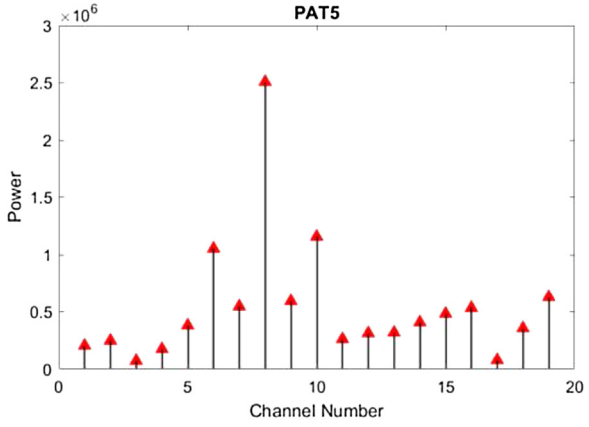

Fig. 13 – Example channel selection (for PAT5).

In Table 7, the performance comparison of the proposed work with other studies is presented.

Since the database used in this work is very comprehensive, electrode type (non-invasive or invasive) and patients differ within the methods proposed in the literature. Looking at the results, the proposed study provides the best FPR performance compared to other studies suggested in the literature and is unique in terms of real-time operation and hardware architecture.

In the proposed study, the earliest estimation time was calculated as 47.6 min, the latest estimation time as 13.28 min, and the average estimation time as 33.23 min. The intervention time was determined as 5 min for all patients. When looking at the results of other studies performed, it is seen that the forecast time to the closest environment to the proposed system is 30 min. In Ref. [37], it is seen that this period is 60 min. In some studies, this period was not calculated. Instead, only the classification is made and the classification results are presented as performance parameters. In the proposed study, when these durations are evaluated, it is evaluated that the intervention time and mean estimation time values can be sufficient for patient safety.

Most of the studies presented in Table 7 were conducted using more than one electrode. In Ref. [52], a neuron hardware architecture is presented that can be utilized in each EEG channel of a seizure prediction system. However, the architecture in Ref. [52] is hard to be considered as a complete seizure prediction hardware since it does not deal with the raw EEG data but a processed one. Thus, neither false positive rate nor prediction time information is provided. In Ref. [81], 67.7% success is achieved by using a single electrode. Different from the method proposed in this study, an ANN-based method has been used there. Also, EEG data of a pediatric patient taken from the Epilepsy Center of Xijing Hospital have been used as the database.

Table 6 – List of Channel Selected.

Patient	Selected Channel
PAT1	T8
PAT2	F7
PAT3	F7
PAT4	F8
PAT5	P4
PAT6	T8
PAT7	T8
PAT8	O1
PAT9	F7
PAT10	T7

Table 7 – Comparison of the proposed method with works.

HW Architecture	DataBase	Number of Channel	Sensitivity (%)	FPR	Mean of Prediction Time (Minutes)	Hardware Implementation	Realtime
[23]	EU	6	10–100	$0.15h^{-1}$	30	No	No
[24]	EU	6	73	$0.15\ h^{-1}$	–	No	No
[22]	EU	6	**75.8**	$0.1\ h^{-1}$	–	No	No
[17]	EU	>1	38.47	$0.20\ h^{-1}$	–	No	No
[77]	EU	15	50–60	$0.15\ h^{-1}$	–	No	No
[15]	Freiburg	4–6	**92.5**	$0.20\ h^{-1}$	–	No	No
[37]	Freiburg	6	**100**	–	**60**	No	Yes
[78]	VGH, CHB,	18	**88.34**	$0.155\ h^{-1}$	22.5	No	No
[79]	FAHMU	5	**94.59**	$0.084\ h^{-1}$	26.64	No	No
[80]	CHB	23	**76**	–	–	No	No
[52]	Bonn	Not Applicable	**90**	Not Applicable	Not Applicable	Yes (Not Complete)	Not Applicable
[14]	CHB	23	**87.26**	0.13%	–	No	No
[81]	ECXH	**1**	67.4	–	–	No	Yes
This Work	**EU**	**1**	**77.3**	**$0.041\ h^{-1}$**	**33.23**	**Yes**	**Yes**

(VGH): Vancouver General Hospital; (FAHMU): First Affiliated Hospital of Xinjiang Medical University; (ECXH): Epilepsy Center of Xijing Hospital; (EU): The European Epilepsy Database.
Bold values signifies that from the results obtained from this study, other results with better results were highlighted.

Apart from these, real-time hardware using a single electrode has been proposed in Ref. [40]. The difference from this study uses the method proposed by itself instead of the machine learning algorithm. It is thought to be an innovative addition to the literature with its simple method and high performance. However, when the study is examined, it is seen that the training data is randomly selected and the same data are used in the test phase. Therefore, SEN and FPR values are considered to be high.

It seems that the average SEN value of the proposed study is lower than some studies presented in Table 7. However, these performance values should be evaluated on a patient basis because epilepsy is a disease with patient-specific characteristics. As seen in Table 4, the sensitivity of the proposed system varies between 50% and 100% when evaluated on a patient basis. Having 50% success in a patient with two attacks means preventing the patient from doing one of the two potentially fatal activities. As a result, the life of the patient is saved once.

A prediction system must have a high SEN value as well as a low FPR. While all attacks are predicted correctly, it is not desired to give the patient a constant false alarm. In the proposed system, FPR is calculated between 0 and $0.136\ h^{-1}$. When the previous studies in Table 7 are examined, it is seen that the rate of FPR is lower than other studies.

Transforming the proposed study into a wearable system will be a comfortable structure for the patient since a single electrode is used. However, the selected channel may not represent future attacks or noise may penetrate the signal of the single-channel selected at SPH + SOP moments. In such a situation, the seizure prediction performance of the proposed system will decrease. Thus, the proposed system is considered to be disadvantageous compared to studies using more than one electrode.

5. Conclusion

In this study, a real-time epileptic seizure prediction algorithm and hardware architecture are proposed. EEG data of 10 patients in ''The European Epilepsy Database'' are used in the study. EEG signals are preprocessed and the first 5 IMFs were calculated and a total of eighty-five features are extracted. Then, the RusBoosted Tree classifier, which can make fast classification, is used and post-processing is applied to the classification results. Finally, alarms are generated for possible seizures by looking at the TH1, TH2, and TH3 threshold values. Unlike previous studies, the prediction process is carried out using a unipolar signal from a single EEG electrode with a machine learning algorithm. As a result of the tests, a real-time seizure prediction algorithm and hardware architecture have been shown to work successfully using single-electrode EEG.

In future studies, considering the development of EEG data acquisition systems, it is considered that a single-channel smooth and noiseless EEG measurement system can be easily integrated into a real-time platform [82,83]. The process of selecting the right EEG probe and defining the threshold values automatically would make the proposed method a generic solution candidate for the patients suffering from epilepsy in a wearable biomedical device form or a cloud-based service form.

Declaration of interests

The authors declare that they have no known competing financial interests or personal relationships that could have appeared to influence the work reported in this paper.

CRediT authorship contribution statement

Ercan Cosgun: Software, Formal analysis, Investigation, Data curation, Resources, Visualization, Writing - original draft. **Anil Çelebi:** Supervision, Methodology, Project administration, Conceptualization, Funding acquisition, Writing - review & editing.

CRediT authorship contribution statement

Ercan Cosgun: Software, Formal analysis, Investigation, Data curation, Resources, Visualization, Writing - original draft. **Anil Çelebi**: Supervision, Methodology, Project administration, Conceptualization, Funding acquisition, Writing - review & editing.

Acknowledgment

This work was supported by Kocaeli University, Scientific Research Projects Coordination Unit, under project number:2018/063. Kuantek Electronics has donated FPGA development board. Xilinx has donated software products under ''Xilinx University Programme''.

REFERENCES

[1] WHO EPILEPSY 2019. https://www.who.int/news-room/fact-sheets/detail/epilepsy.
[2] Zack MM, Kobau R. National and state estimates of the numbers of adults and children with active epilepsy — united States, 2015. Morb Mortal Wkly Rep Surveill Summ 2017;66:821–5. http://dx.doi.org/10.15585/mmwr.mm6631a1
[3] Rogers SL, Buzsáki G. What is epilepsy and how can you help someone with it? Front Young Minds 2019;7:1–7. http://dx.doi.org/10.3389/frym.2019.00052
[4] Rao S, Stino A, Seraji-Bozorgzad N, Shah AK, Basha MM. Seizure-related injury and postictal aggression in refractory epilepsy patients. Epilepsy Res 2020;160106281. http://dx.doi.org/10.1016/j.eplepsyres.2020.106281
[5] Bandarabadi M, Rasekhi J, Teixeira CA, Karami MR, Dourado A. On the proper selection of preictal period for seizure prediction. Epilepsy Behav 2015;46:158–66. http://dx.doi.org/10.1016/j.yebeh.2015.03.010
[6] Asharindavida F, Shamim Hossain M, Thacham A, Khammari H, Ahmed I, Alraddady F, et al. A forecasting tool for prediction of epileptic seizures using a machine learning approach. Concurr Comput 2020;32:1–24. http://dx.doi.org/10.1002/cpe.5111
[7] Zhang Z, Parhi KK. Low-complexity seizure prediction from iEEG/sEEG using spectral power and ratios of spectral power. IEEE Trans Biomed Circuits Syst 2016;10:693–706. http://dx.doi.org/10.1109/TBCAS.2015.2477264
[8] Ramina P, Vanitha M, Professor A. Fast and effective real time seizure prediction on streaming EEG signals. Int J Electron Commun Instrum Eng Res Dev 2017;9:167–79.
[9] Alickovic E, Kevric J, Subasi A. Performance evaluation of empirical mode decomposition, discrete wavelet transform, and wavelet packed decomposition for automated epileptic seizure detection and prediction. Biomed Signal Process Control 2018;39:94–102. http://dx.doi.org/10.1016/j.bspc.2017.07.022
[10] Wilson SB, Scheuer ML, Plummer C, Young B, Pacia S. Seizure detection: correlation of human experts. Clin Neurophysiol 2003;114:2156–64. http://dx.doi.org/10.1016/S1388-2457(03)00212-8
[11] Zhang Q, Hu Y, Potter T, Li R, Quach M, Zhang Y. Establishing functional brain networks using a nonlinear partial directed coherence method to predict epileptic seizures. J Neurosci Methods 2020;329108447. http://dx.doi.org/10.1016/j.jneumeth.2019.108447
[12] Yu Z, Nie W, Zhou W, Xu F, Yuan S, Leng Y, et al. Epileptic seizure prediction based on local mean decomposition and deep convolutional neural network. J Supercomput 2018. http://dx.doi.org/10.1007/s11227-018-2600-6
[13] Bigelow MD, Kouzani AZ. Neural stimulation systems for the control of refractory epilepsy: a review. J Neuroeng Rehabil 2019;16:1–17. http://dx.doi.org/10.1186/s12984-019-0605-x
[14] Agboola HA, Solebo C, Aribike DS, Lesi AE, Susu A. Seizure prediction with adaptive feature representation learning. J Neurol Neurosci 2019;10:1–12. http://dx.doi.org/10.36648/2171-6625.10.2.294
[15] Park Y, Luo L, Parhi KK, Netoff T. Seizure prediction with spectral power of EEG using cost-sensitive support vector machines. Epilepsia 2011;52:1761–70. http://dx.doi.org/10.1111/j.1528-1167.2011.03138.x
[16] Rukhsar S, Khan YU, Farooq O, Sarfraz M, Khan AT. Patient-specific epileptic seizure prediction in long-term scalp EEG signal using multivariate statistical process control. Irbm 2019;40:320–31. http://dx.doi.org/10.1016/j.irbm.2019.08.004
[17] Direito B, Teixeira CA, Sales F, Castelo-Branco M, Dourado A. A realistic seizure prediction study based on multiclass SVM. Int J Neural Syst 2017;27. http://dx.doi.org/10.1142/S012906571750006X
[18] Truong ND, Nguyen AD, Kuhlmann L, Bonyadi MR, Yang J, Ippolito S, et al. Convolutional neural networks for seizure prediction using intracranial and scalp electroencephalogram. Neural Netw 2018;105:104–11. http://dx.doi.org/10.1016/j.neunet.2018.04.018
[19] Sharif B, Jafari AH. Prediction of epileptic seizures from EEG using analysis of ictal rules on Poincaré plane. Comput Methods Programs Biomed 2017;145:11–22. http://dx.doi.org/10.1016/j.cmpb.2017.04.001
[20] D'Alessandro M, Esteller R, Echauz J, Vachtsevanos G, Hinson A, Litt B. Epileptic seizure prediction using hybrid feature selection over multiple intracranial EEG electrode contacts: a report of four patients. IEEE Trans Biomed Eng 2003;50:603–15. http://dx.doi.org/10.1109/TBME.2003.810706
[21] Li Q, Gao J, Zhang Z, Huang Q, Wu Y, Xu B. Distinguishing epileptiform discharges from normal electroencephalograms using adaptive fractal and network analysis: a clinical perspective. Front Physiol 2020;11:1–15. http://dx.doi.org/10.3389/fphys.2020.00828
[22] Bandarabadi M, Teixeira CA, Rasekhi J, Dourado A. Epileptic seizure prediction using relative spectral power features. Clin Neurophysiol 2015;126:237–48. http://dx.doi.org/10.1016/j.clinph.2014.05.022
[23] Alexandre Teixeira C, Direito B, Bandarabadi M, Le Van Quyen M, Valderrama M, Schelter B, et al. Epileptic seizure predictors based on computational intelligence techniques: a comparative study with 278 patients. Comput Methods Programs Biomed 2014;114:324–36. http://dx.doi.org/10.1016/j.cmpb.2014.02.007
[24] Rasekhi J, Mollaei MRK, Bandarabadi M, Teixeira CA, Dourado A. Preprocessing effects of 22 linear univariate features on the performance of seizure prediction methods. J Neurosci Methods 2013;217:9–16. http://dx.doi.org/10.1016/j.jneumeth.2013.03.019
[25] Quintero-Rincón A, Pereyra M, D'Giano C, Risk M, Batatia H. Fast statistical model-based classification of epileptic EEG signals. Biocybern Biomed Eng 2018;38:877–89. http://dx.doi.org/10.1016/j.bbe.2018.08.002
[26] Sudalaimani C, Sivakumaran N, Elizabeth TT, Rominus VS. Automated detection of the preseizure state in EEG signal using neural networks. Biocybern Biomed Eng 2019;39:160–75. http://dx.doi.org/10.1016/j.bbe.2018.11.007

[27] Khan H, Marcuse L, Fields M, Swann K, Yener B. Focal onset seizure prediction using convolutional networks. IEEE Trans Biomed Eng 2018;65:2109–18. http://dx.doi.org/10.1109/TBME.2017.2785401
[28] Tzallas AT, Tsipouras MG, Fotiadis DI. Epileptic seizure detection in EEGs using time-frequency analysis. IEEE Trans Inf Technol Biomed 2009;13:703–10. http://dx.doi.org/10.1109/TITB.2009.2017939
[29] Samiee K, Kovács P, Gabbouj M. Epileptic seizure detection in long-term EEG records using sparse rational decomposition and local Gabor binary patterns feature extraction. Knowledge-Based Syst 2017;118:228–40. http://dx.doi.org/10.1016/j.knosys.2016.11.023
[30] Yu H, Fan C, Zhang Y, Huang C. Epilepsy detection in EEG using grassmann discriminant analysis method. Comput Math Methods Med 2020;2020. http://dx.doi.org/10.1155/2020/2598140
[31] Chen G, Xie W, Bui TD, Krzyzak A. Automatic epileptic seizure detection in EEG using nonsubsampled wavelet–Fourier features. J Med Biol Eng 2017;37:123–31. http://dx.doi.org/10.1007/s40846-016-0214-0
[32] Krishnan PT, Joseph Raj AN, Balasubramanian P, Chen Y. Schizophrenia detection using MultivariateEmpirical Mode Decomposition and entropy measures from multichannel EEG signal. Biocybern Biomed Eng 2020;40:1124–39. http://dx.doi.org/10.1016/j.bbe.2020.05.008
[33] Usman SM, Usman M, Fong S. Epileptic seizures prediction using machine learning methods. Comput Math Methods Med 2017;2017. http://dx.doi.org/10.1155/2017/9074759
[34] Bishop CM. Pattern recognition and machine learning;New York, NY 2006.
[35] Hu W, Cao J, Lai X, Liu J. Mean amplitude spectrum based epileptic state classification for seizure prediction using convolutional neural networks. J Ambient Intell Humaniz Comput 2019;0:0. http://dx.doi.org/10.1007/s12652-019-01220-6
[36] Dhiman R, Saini JS, Priyanka. Genetic algorithms tuned expert model for detection of epileptic seizures from EEG signatures. Appl Soft Comput J 2014;19:8–17. http://dx.doi.org/10.1016/j.asoc.2014.01.029
[37] Chisci L, Mavino A, Perferi G, Sciandrone M, Anile C, Colicchio G, et al. Real-time epileptic seizure prediction using AR models and support vector machines. IEEE Trans Biomed Eng 2010;57:1124–32. http://dx.doi.org/10.1109/TBME.2009.2038990
[38] Ibrahim S, Djemal R, Alsuwailem A. Electroencephalography (EEG) signal processing for epilepsy and autism spectrum disorder diagnosis. Biocybern Biomed Eng 2018;38:16–26. http://dx.doi.org/10.1016/j.bbe.2017.08.006
[39] Wang L, Wang C, Fu F, Yu X, Guo H, Xu C, et al. Temporal lobe seizure prediction based on a complex Gaussian wavelet. Clin Neurophysiol 2011;122:656–63. http://dx.doi.org/10.1016/j.clinph.2010.09.018
[40] Sadeghzadeh H, Hosseini-Nejad H, Salehi S. Real-time epileptic seizure prediction based on online monitoring of pre-ictal features. Med Biol Eng Comput 2019;57:2461–9. http://dx.doi.org/10.1007/s11517-019-02039-1
[41] Savadkoohi M, Oladunni T, Thompson L. A machine learning approach to epileptic seizure prediction using Electroencephalogram (EEG) Signal. Biocybern Biomed Eng 2020;40:1328–41. http://dx.doi.org/10.1016/j.bbe.2020.07.004
[42] Li M, Chen W, Zhang T. Automatic epilepsy detection using wavelet-based nonlinear analysis and optimized SVM. Biocybern Biomed Eng 2016;36:708–18. http://dx.doi.org/10.1016/j.bbe.2016.07.004
[43] Xiang J, Li C, Li H, Cao R, Wang B, Han X, et al. The detection of epileptic seizure signals based on fuzzy entropy. J Neurosci Methods 2015;243:18–25. http://dx.doi.org/10.1016/j.jneumeth.2015.01.015
[44] Mamli S, Kalbkhani H. Gray-level co-occurrence matrix of Fourier synchro-squeezed transform for epileptic seizure detection. Biocybern Biomed Eng 2019;39:87–99. http://dx.doi.org/10.1016/j.bbe.2018.10.006
[45] Li M, Chen W, Zhang T. Automatic epileptic EEG detection using DT-CWT-based non-linear features. Biomed Signal Process Control 2017;34:114–25. http://dx.doi.org/10.1016/j.bspc.2017.01.010
[46] Zhang T, Chen W, Li M. Generalized Stockwell transform and SVD-based epileptic seizure detection in EEG using random forest. Biocybern Biomed Eng 2018;38:519–34. http://dx.doi.org/10.1016/j.bbe.2018.03.007
[47] Li M, Chen W, Zhang T. Application of MODWT and log-normal distribution model for automatic epilepsy identification. Biocybern Biomed Eng 2017;37:679–89. http://dx.doi.org/10.1016/j.bbe.2017.08.003
[48] Li M, Chen W, Zhang T. Classification of epilepsy EEG signals using DWT-based envelope analysis and neural network ensemble. Biomed Signal Process Control 2017;31:357–65. http://dx.doi.org/10.1016/j.bspc.2016.09.008
[49] Solaija MSJ, Saleem S, Khurshid K, Hassan SA, Kamboh AM. Dynamic mode decomposition based epileptic seizure detection from scalp EEG. IEEE Access 2018;6:38683–92. http://dx.doi.org/10.1109/ACCESS.2018.2853125
[50] Das K, Daschakladar D, Roy PP, Chatterjee A, Saha SP. Epileptic seizure prediction by the detection of seizure waveform from the pre-ictal phase of EEG signal. Biomed Signal Process Control 2020;57101720. http://dx.doi.org/10.1016/j.bspc.2019.101720
[51] Burrello A, Schindler K, Benini L, Rahimi A. One-shot learning for iEEG seizure detection using end-to-end binary operations: local binary patterns with hyperdimensional computing. ArXiv 2018.
[52] Kueh SM, Kazmierski TJ. Low-power and low-cost dedicated bit-serial hardware neural network for epileptic seizure prediction system. IEEE J Transl Eng Heal Med 2018;6. http://dx.doi.org/10.1109/JTEHM.2018.2867864
[53] Safaei A, Wu QMJ, Yang Y. System-on-a-chip (SoC)-based hardware acceleration for foreground and background identification. J Franklin Inst 2018;355:1888–912. http://dx.doi.org/10.1016/j.jfranklin.2017.07.037
[54] Kocaoglu S, Akdogan E. Design and development of an intelligent biomechatronic tumor prosthesis. Biocybern Biomed Eng 2019;39:561–70. http://dx.doi.org/10.1016/j.bbe.2019.05.004
[55] Karpova EV, Karyakin EE, Karyakin AA. Wearable non-invasive monitors of diabetes and hypoxia through continuous analysis of sweat. Talanta 2020;215120922. http://dx.doi.org/10.1016/j.talanta.2020.120922
[56] Bent B, Goldstein BA, Kibbe WA, Dunn JP. Investigating sources of inaccuracy in wearable optical heart rate sensors. Npj Digit Med 2020;3:1–9. http://dx.doi.org/10.1038/s41746-020-0226-6
[57] Teohari VM, Ungureanu C, Bui V, Arends JBAM, Aarts RM. Epilepsy seizure detection app for wearable technologies; 2014. pp. 1–6.
[58] Iranmanesh S, Raikos G, Imtiaz SA, Rodriguez-Villegas E. A seizure-based power reduction SoC for wearable EEG in epilepsy. IEEE Access 2019;7:151682–91. http://dx.doi.org/10.1109/ACCESS.2019.2948231
[59] Gu Y, Cleeren E, Dan J, Claes K, Van Paesschen W, Van Huffel S, et al. Comparison between scalp EEG and behind-the-ear EEG for development of a wearable seizure detection system for patients with focal epilepsy. Sensors

(Switzerland) 2018;18:1–17. http://dx.doi.org/10.3390/s18010029
[60] Imtiaz SA, Logesparan L, Rodriguez-Villegas E. Performance-power consumption tradeoff in wearable epilepsy monitoring systems. IEEE J Biomed Heal Informatics 2015;19:1019–28. http://dx.doi.org/10.1109/JBHI.2014.2342501
[61] Meisel C, El Atrache R, Jackson M, Schubach S, Ufongene C, Loddenkemper T. Machine learning from wristband sensor data for wearable, noninvasive seizure forecasting. Epilepsia 2020. http://dx.doi.org/10.1111/epi.16719
[62] Ihle M, Feldwisch-Drentrup H, Teixeira CA, Witon A, Schelter B, Timmer J, et al. EPILEPSIAE - A European epilepsy database. Comput Methods Programs Biomed 2012;106:127–38. http://dx.doi.org/10.1016/j.cmpb.2010.08.011
[63] Truong ND, Kuhlmann L, Bonyadi MR, Querlioz D, Zhou L, Kavehei O. Epileptic seizure forecasting with generative adversarial networks. IEEE Access 2019;7:143999–4009. http://dx.doi.org/10.1109/ACCESS.2019.2944691
[64] European Epilepsy Database 2012. http://epilepsy-database.eu/ (accessed June 30, 2020).
[65] Huang NE, Shen Z, Long SR, Wu MC, Snin HH, Zheng Q, et al. The empirical mode decomposition and the Hubert spectrum for nonlinear and non-stationary time series analysis. Proc R Soc A Math Phys Eng Sci 1998;454:903–95. http://dx.doi.org/10.1098/rspa.1998.0193
[66] Gul S, Siddiqui MF, Ur Rehman N. FPGA based real-time implementation of online EMD with fixed point architecture. IEEE Access 2019;7:176565–77. http://dx.doi.org/10.1109/ACCESS.2019.2957819
[67] Wang G, Chen XY, Qiao FL, Wu Z, Huang NE. On intrinsic mode function. Adv Adapt Data Anal 2010;2:277–93. http://dx.doi.org/10.1142/S1793536910000549
[68] Huang NE, Shen Z, Long SR, Wu MC, Shih HH, Zheng Q, et al. The empirical mode decomposition and the Hilbert spectrum for nonlinear and non-stationary time series analysis. Proc R Soc London Ser A Math Phys Eng Sci 1998;454:903–95. http://dx.doi.org/10.1098/rspa.1998.0193
[69] Rato RT, Ortigueira MD, Batista AG. On the HHT, its problems, and some solutions. Mech Syst Signal Process 2008;22:1374–94. http://dx.doi.org/10.1016/j.ymssp.2007.11.028
[70] Karabiber Cura O, Kocaaslan Atli S, Türe HS, Akan A. Epileptic seizure classifications using empirical mode decomposition and its derivative. Biomed Eng Online 2020;19:10. http://dx.doi.org/10.1186/s12938-020-0754-y
[71] Sankari ES, Manimegalai D. Predicting membrane protein types using various decision tree classifiers based on various modes of general PseAAC for imbalanced datasets. J Theor Biol 2017;435:208–17. http://dx.doi.org/10.1016/j.jtbi.2017.09.018
[72] Lim Chee-Keong Alfred, Chia WC. Analysis of single-electrode EEG rhythms using MATLAB to elicit correlation with cognitive stress. Int J Comput Theory Eng 2015;7:149–55. http://dx.doi.org/10.7763/IJCTE.2015.V7.947
[73] Jain G, Mittal D, Thakur D, Mittal MK. A deep learning approach to detect Covid-19 coronavirus with X-Ray images. Biocybern Biomed Eng 2020;40:1391–405. http://dx.doi.org/10.1016/j.bbe.2020.08.008
[74] Seiffert C, Khoshgoftaar TM, Van Hulse J, Napolitano A. RUSBoost: A hybrid approach to alleviating class imbalance. IEEE Trans Syst Man Cybern Part ASystems Humans 2010;40:185–97. http://dx.doi.org/10.1109/TSMCA.2009.2029559
[75] Spring D. On the second derivative test for constrained local extrema. Am Math Mon 1985;92:631–43. http://dx.doi.org/10.1080/00029890.1985.11971702
[76] Faires RB. J. Numerical analysis. ninth edit. BROOKS/COLE; 2010.
[77] Feldwisch-Drentrup H, Ihle M, le van Quyen M, Teixeira C, Dourado A, Timmer J, et al. Anticipating the unobserved: prediction of subclinical seizures. Epilepsy Behav 2011;22: S119–26. http://dx.doi.org/10.1016/j.yebeh.2011.08.023
[78] Zandi AS, Tafreshi R, Javidan M, Dumont GA. Predicting epileptic seizures in scalp EEG based on a variational bayesian gaussian mixture model of zero-crossing intervals. IEEE Trans Biomed Eng 2013;60:1401–13. http://dx.doi.org/10.1109/TBME.2012.2237399
[79] Zhang Z, Chen Z, Zhou Y, Du S, Zhang Y, Mei T, et al. Construction of rules for seizure prediction based on approximate entropy. Clin Neurophysiol 2014;125:1959–66. http://dx.doi.org/10.1016/j.clinph.2014.02.017
[80] Ibrahim SW, Djemal R, Alsuwailem A, Gannouni S. Electroencephalography (EEG)-based epileptic seizure prediction using entropy and K-nearest neighbor (KNN). Commun Sci Technol 2017;2:6–10. http://dx.doi.org/10.21924/cst.2.1.2017.44
[81] Zhu T, Huang L, Tian X. Epileptic seizure prediction by using empirical mode decomposition and complexity analysis of single-channel scalp electroencephalogram. Proc 2009 2nd Int Conf Biomed Eng Informatics; 2009. pp. 1–4. http://dx.doi.org/10.1109/BMEI.2009.5305382
[82] Kappel SL, Rank ML, Toft HO, Andersen M, Kidmose P. Dry-contact electrode Ear-EEG. IEEE Trans Biomed Eng 2019;66:150–8. http://dx.doi.org/10.1109/TBME.2018.2835778
[83] Yin L, Zhang C, Cui Z. Experimental research on real-time acquisition and monitoring of wearable EEG based on TGAM module. Comput Commun 2020;151:76–85. http://dx.doi.org/10.1016/j.comcom.2019.12.055